Supporting information for:

A Water-soluble BODIPY Based 'OFF/ON' Fluorescence Probe for the Detection of Cd^{2+} Ions with High Selectivity and Sensitivity

Apurba Maity,[a] Utsav Ghosh,[a] Dipanjan Giri,[a] Devdeep Mukherjee,[b] Tapas Kumar Maiti,[b] Sanjib K. Patra*[a]

[a]*Department of Chemistry, Indian Institute of Technology Kharagpur, Kharagpur-721302, WB, INDIA, E-mail: skpatra@chem.iitkgp.ac.in; Tel: +913222283338*

[b]*Department of Biotechnology, Indian Institute of Technology Kharagpur, Kharagpur-721302, WB, INDIA*

1. Synthetic and Characterization

1.a) Synthesis

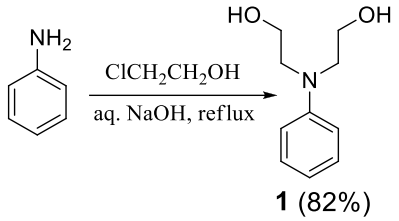

1 (82%)

Scheme 1: synthesis of compound **1**.

N,N-Bis (2-hydroxyethyl) aniline (1):[1] A Schlenk flask was charged with distilled aniline (2.55 g, 0.027 mol) and 2-chlorohydrine (5.51 g, 0.067 mol) and then refluxed while 10% aq NaOH (22 ml) was slowly added. The reaction mixture was then refluxed for overnight. The progess of the reaction was monitored by thin layer chromatography (TLC). After the reaction was completed, the mixture was cooled to room temperature. The reaction mixture was extracted by ethyl acetate and then the organic part was washed with brine. The collected organic layer was dried over anhydrous sodium sulphate, the solvent was removed by rotary evaporation. The crude product was purified by column chromatography using silica gel (60-120 mesh) & 50% ETOAC in hexane as eluent to afford pure compound **1** in yellow solid (4.01 gm, yield 82%). ^{1}H NMR (400MHz, $CDCl_3$): δ 7.21-7.25 (m, 2H, Ph), 6.69-6.76 (m, 3H, Ph), 3.84 (t, J = 4Hz, 4H , -NCH_2), 3.57 (t, J = 4Hz, 4H, -OCH_2).^{13}C{^{1}H} NMR (100MHz, $CDCl_3$): δ 148.0, 129.5, 117.1, 112.8 (Ph), 60.9 (-NCH_2), 55.6 (-OCH_2). FTIR (KBr, cm^{-1}): 3326 ($\nu_{0\text{-H, stretching}}$). MALDI-TOF MS: (m/z) calcd for $C_{10}H_{16}NO_2$ $[M+H]^+$, 182.243; found, 182.553.

Diethyl 2,2'-(2,2'-(phenylazanediyl)bis(ethane-2,1-diyl)bis(oxy))diacetate (2):[2] A 250 ml Schlenk flask was charged with 2 g (11.03 mmol) of N,N-Bis (2-hydroxyethyl) aniline under argon atmosphere. It was kept on an ice bath and 0.97 g (24.26 mmol) NaH (60 % dispersion in mineral oil) was added to it followed by addition of 50 ml THF. Lastly, 2.43 ml (22.1 mmol) of ethyl bromoacetate was added. The resulting reaction mixture was refluxed for 18 hrs at 60˚C. After cooling down to room temperature, filtration was done to remove the solid residue. The solvent was removed under reduced pressure and the residue was extracted with DCM and dried over Na_2SO_4 and concentrated in vacuo. The crude product obtained was purified by silica gel chromatography with 35% EtOAc in

hexane as eluent to give a yellow liquid (2.9 g) in 75% yield. ^{1}H NMR (400MHz, $CDCl_3$): δ 1.27 (t, *J* = 8Hz, 6H), 3.64-3.72 (m, 4H), 4.07 (s, 4H), 4.20 (q, *J* = 8Hz, 4H), 6.66-6.73 (m, 3H), 7.19-7.22 (m, 2H). ^{13}C{^{1}H} NMR (100MHz, $CDCl_3$): δ 14.3, 51.2, 60.1, 68.8, 69.1, 112.1, 116.6, 129.5, 147.7, 170.5. FTIR (KBr, cm^{-1}): 1731 ($\nu_{C=0,\ stretching}$, ester). ESI-MS (*m/z*): calcd for $C_{18}H_{28}NO_6$ $[M+H]^+$, 354.19; found, 354.20.

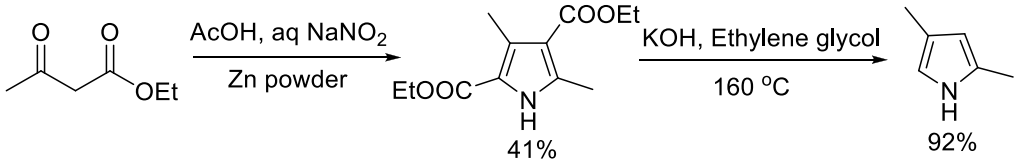

Scheme 2: synthetic route for 2,4-dimethylpyrrole.

Diethyl 3,5-dimethyl-1H-pyrrole-2,4-dicarboxylate:[3] An aqueous solution of sodium nitrite (5.4 g, 78.4 mmol) in water (10 mL) was added to a mixture of ethyl acetoacetic ester (20.4 gm, 20 mL, 156.8 mmol) and acetic acid (40 mL) over 30 min under ice cool condition to keep the temperature below 10 °C. The yellowish clear solution was formed which was allowed to stir for another 2.5 h at 10°C to complete the reaction. Then zinc powder (9.60 g, 156.8 mmol) was added to this mixture portion wise while the reaction mixture was kept below 25°C. Next the reaction mixture was heated to 45–50°C for 10 min and then continued to 95 °C for another 1 h. After cooling down to room temperature yellowish precipitate was formed which was filtered off and washed with ice water (100 mL) to remove the AcOH. The yellow crude solid was recrystallized from ethanol to afford the pure compound as pale yellow crystalline powder (15.4 gm, 41%). ^{1}H NMR (400 MHz $CDCl_3$) δ: (ppm): 8.90 (br s, 1H, pyrrole N-H), 4.35-4.26 (m, 4H, ester O-CH_2), 2,56 (s, 3H, pyrrole-CH_3), 2.51 (s, 3H, pyrrole-CH_3), 1.38-1.34(m, 6H, ester CH_3).

2,4-Dimethyl-1H-pyrrole:[4] In a 250ml schlenk flask purged with argon, compound **1** (2.0g, 8.35 mmol), KOH (2.34g, 41.8 mmol) were charged and heated to reflux in ethylene glycol (15 mL) for 4 hours at 160 °C. After cooling to room temperature, the reaction mixture was extracted with $CHCl_3$, washed with brine solution and dried over Na_2SO_4. The solvent was removed by rotary evaporation to furnish the compound as dark brown oil (0.73 gm, 92%) which was used without further purification. ^{1}H NMR (400 MHz $CDCl_3$) δ(ppm): 7.62 (br s, 1H, pyrrole N-H), 6.41 (s, 1H, pyrrole H), 5.75 (s, 1H, pyrrole H), 2.24 (s, 3H, pyrrole-CH_3), 2.08 (s, 3H, pyrrole-CH_3).

1.b. NMR Spectra

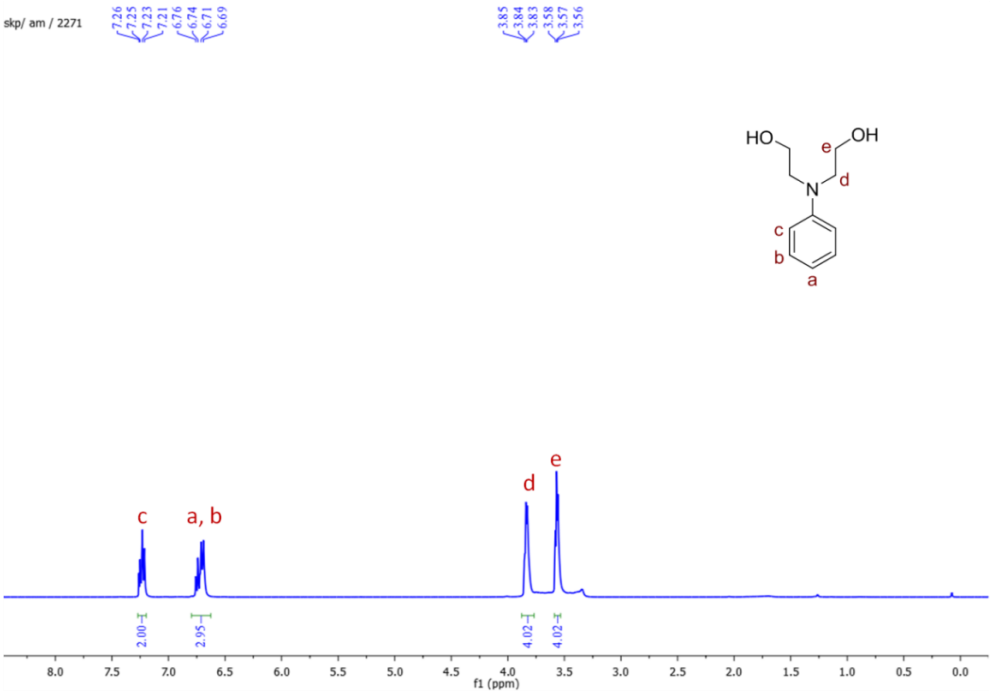

Fig S1: ^{1}H NMR (400 MHz, $CDCl_3$) spectrum of **1**.

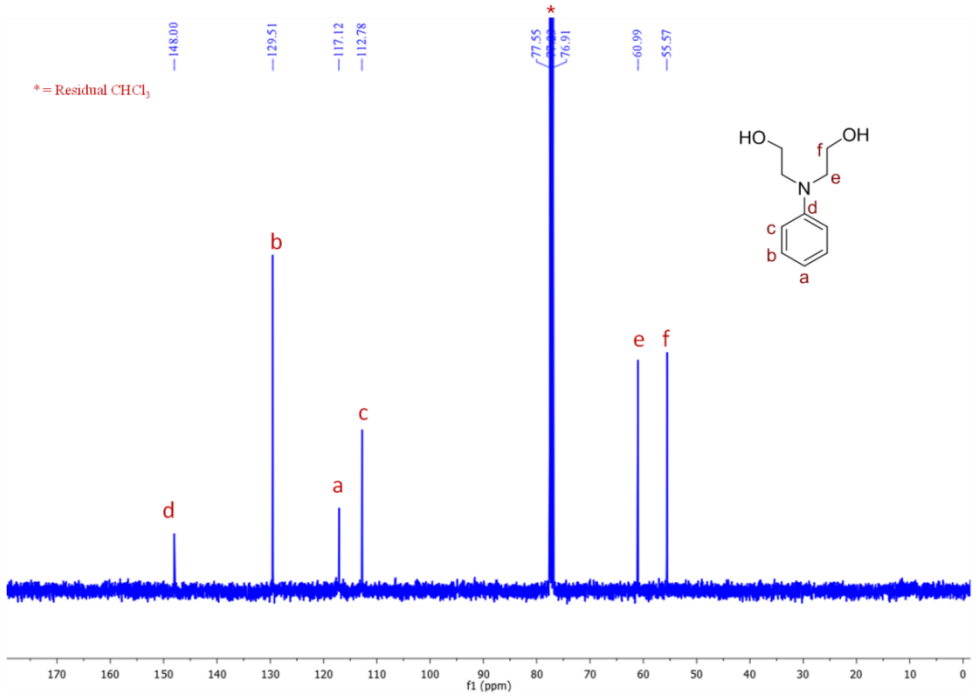

Fig S2: $^{13}C\{^{1}H\}$NMR (100 MHz, $CDCl_3$) spectrum of **1**

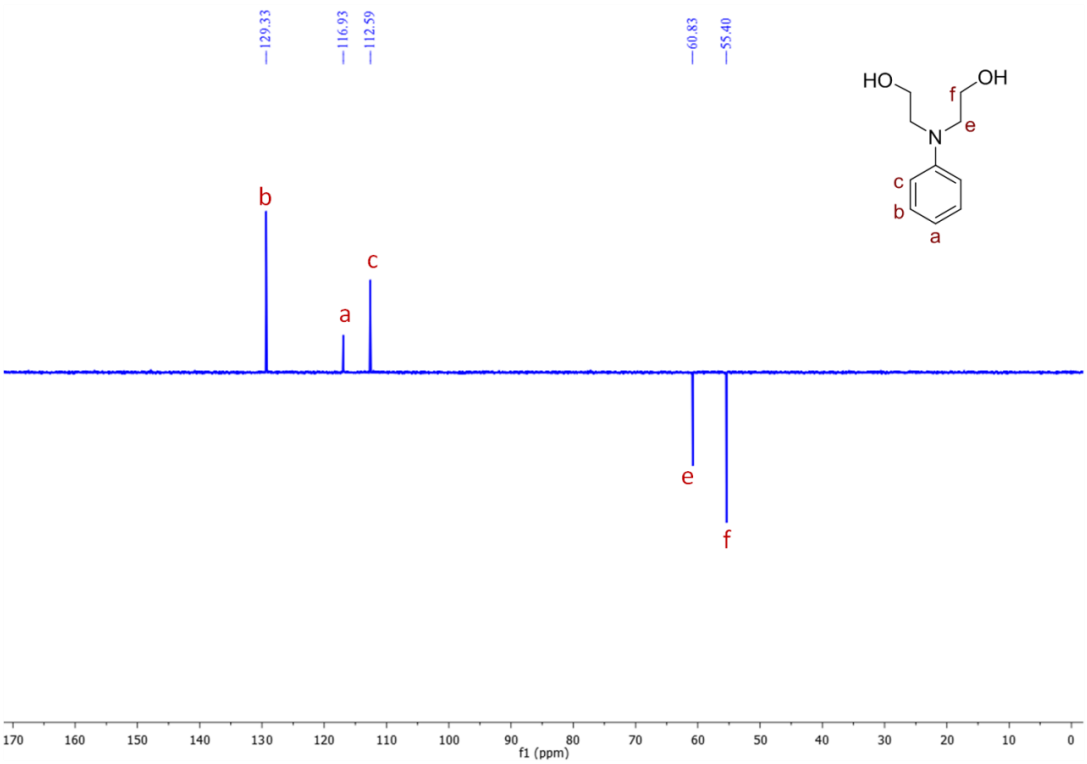

Fig S3: DEPT-135 NMR (100 MHz, $CDCl_3$) spectrum of **1**

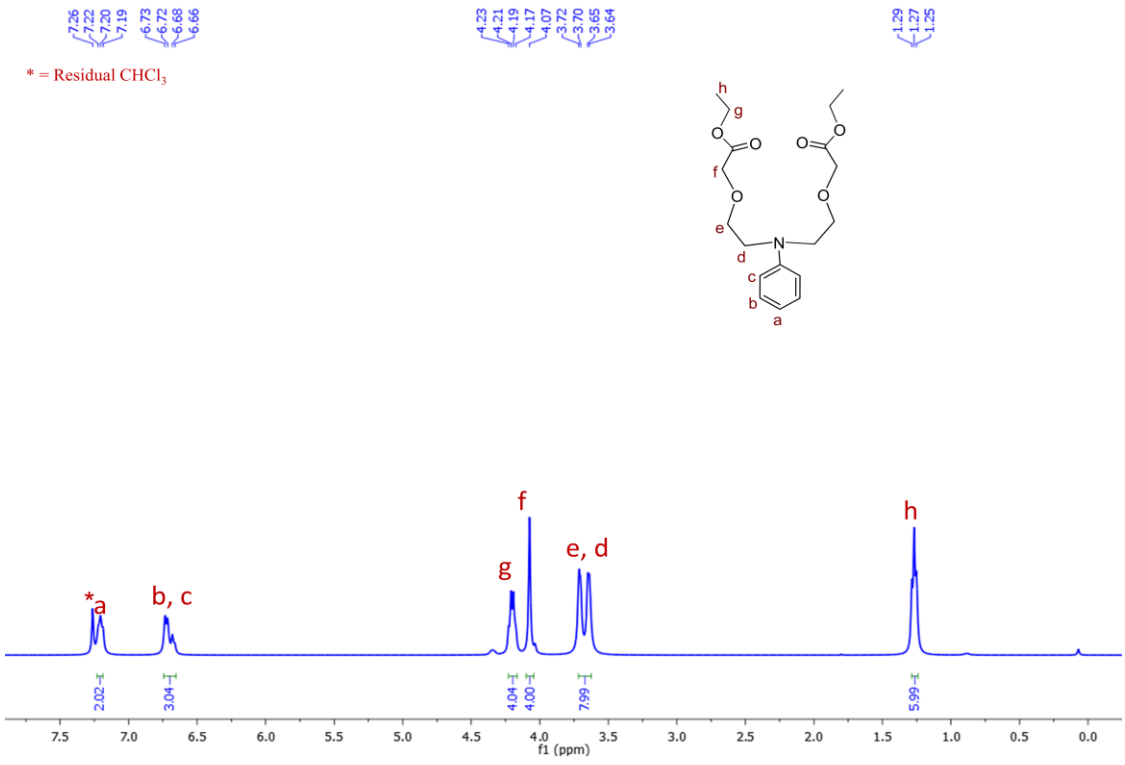

Fig S4: ^1H NMR (400 MHz, $CDCl_3$) spectrum of **2**.

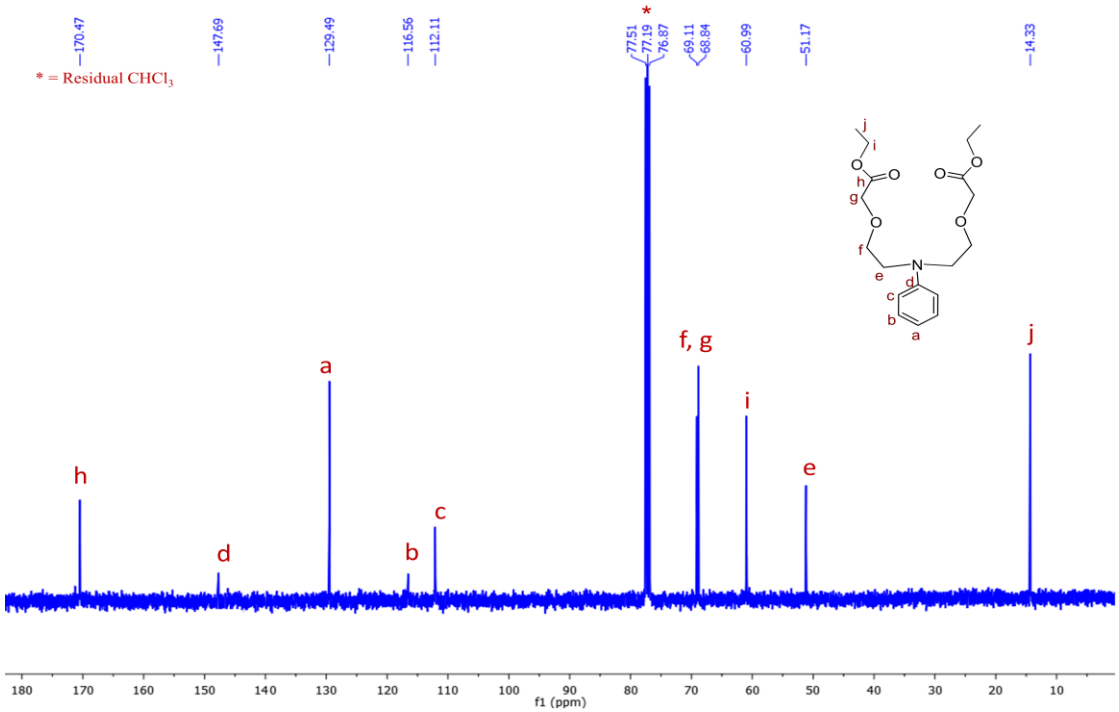

Fig S5: $^{13}C\{^{1}H\}$NMR (100 MHz, $CDCl_3$) spectrum of **2**.

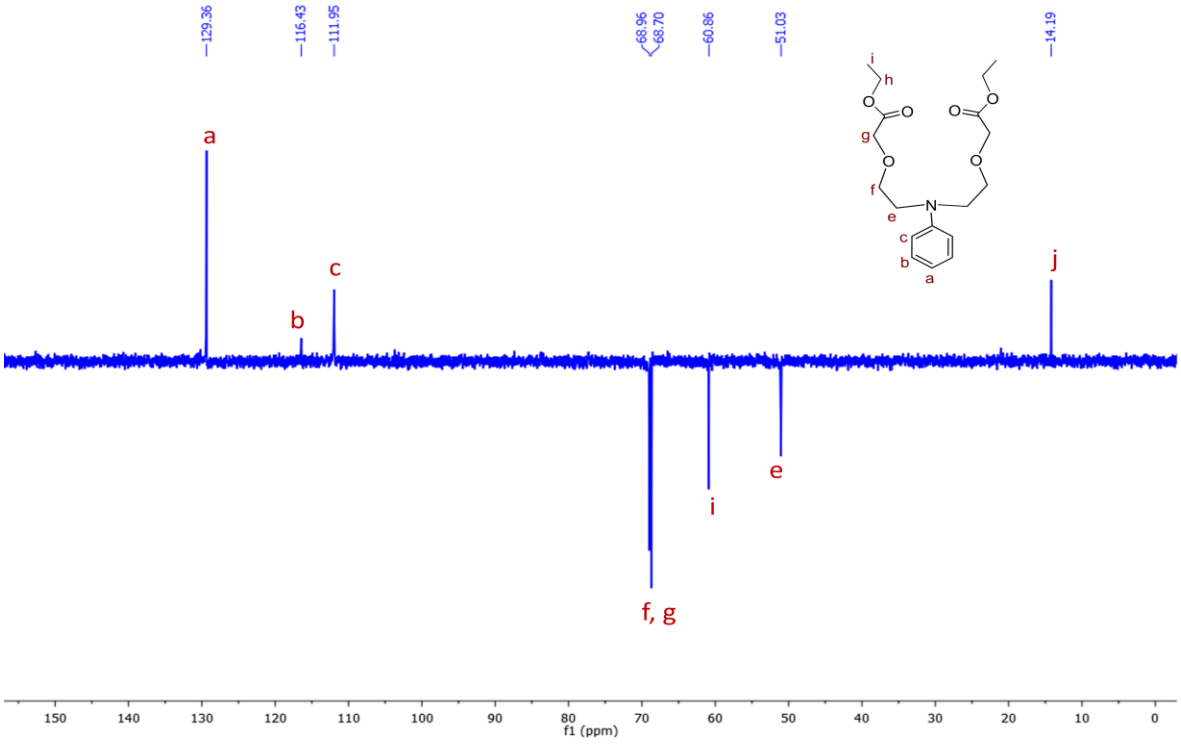

Fig S6: DEPT-135 NMR (100 MHz, $CDCl_3$) spectrum of **2**.

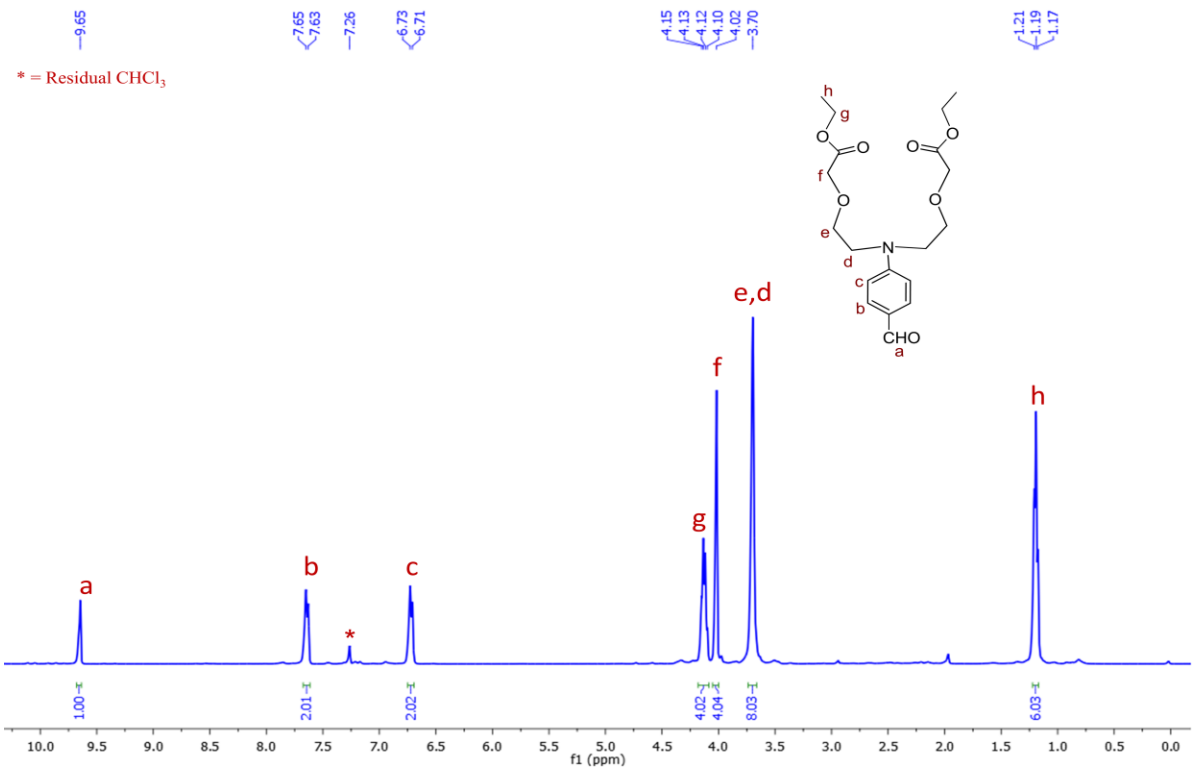

Fig S7: ^{1}H NMR (400 MHz, $CDCl_3$) spectrum of **3**.

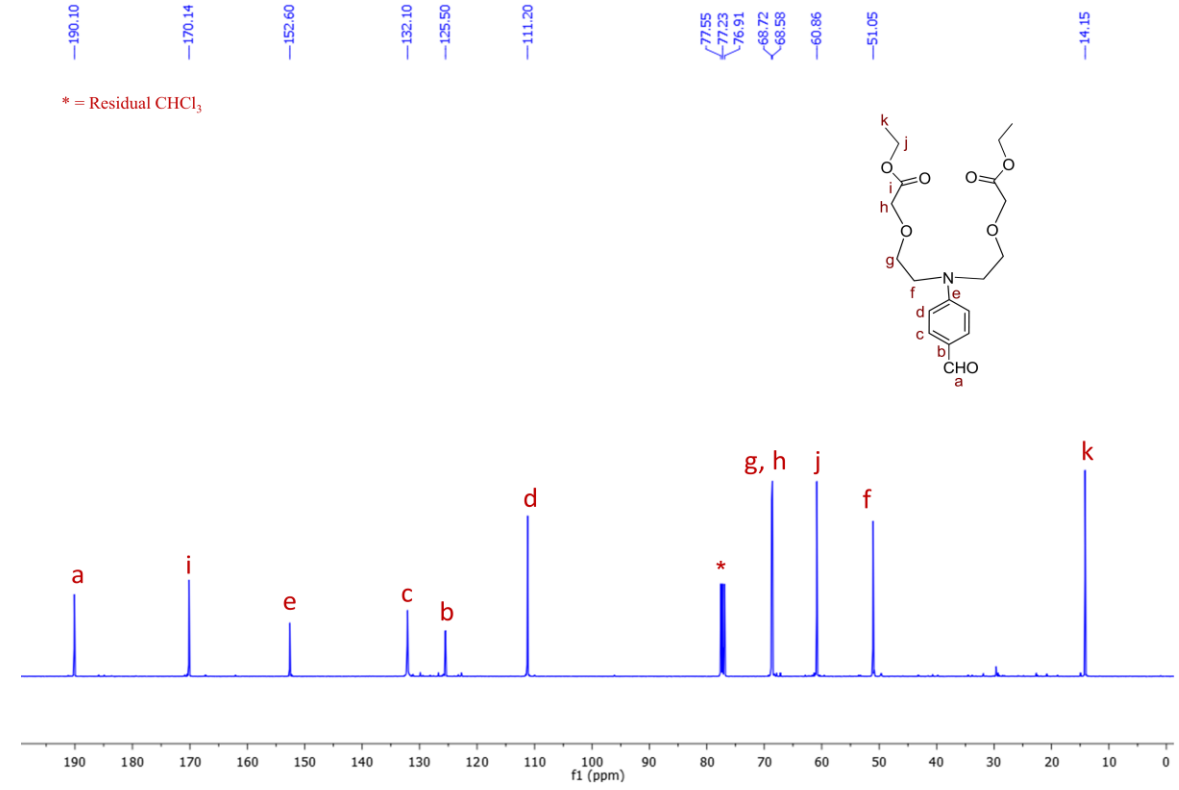

Fig S8: ^{13}C{^{1}H}NMR (100 MHz, $CDCl_3$) spectrum of **3**.

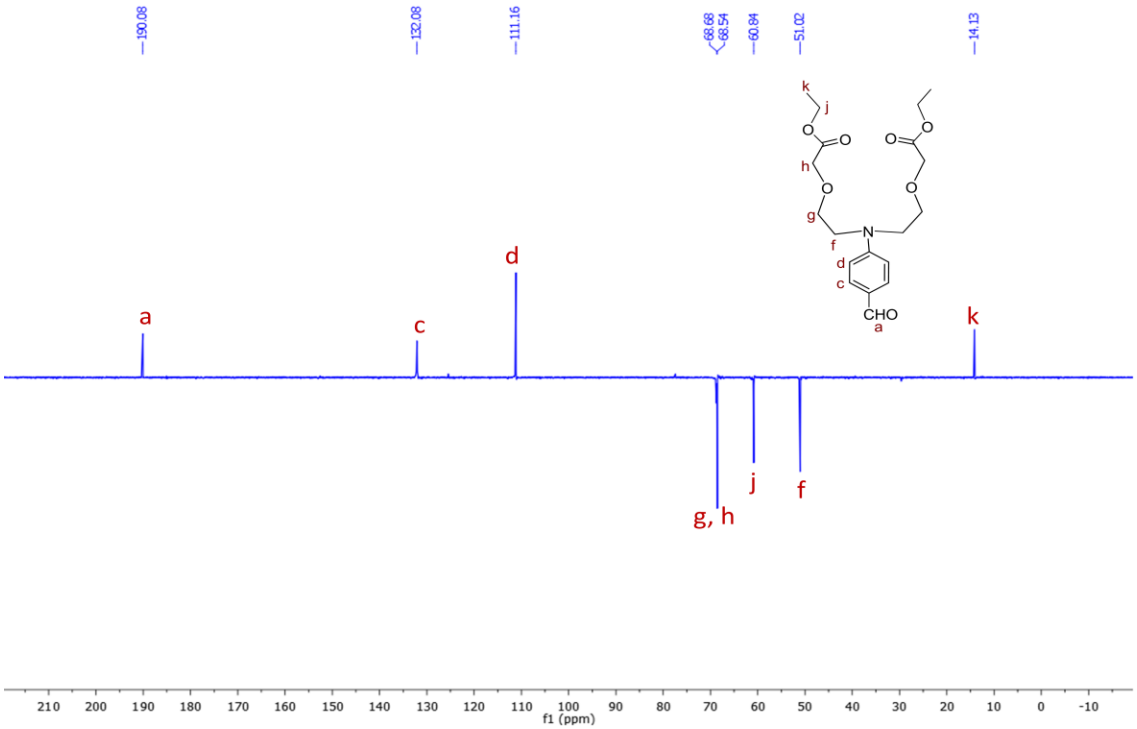

Fig S9: DEPT-135 NMR (100 MHz, $CDCl_3$) spectrum of **3**.

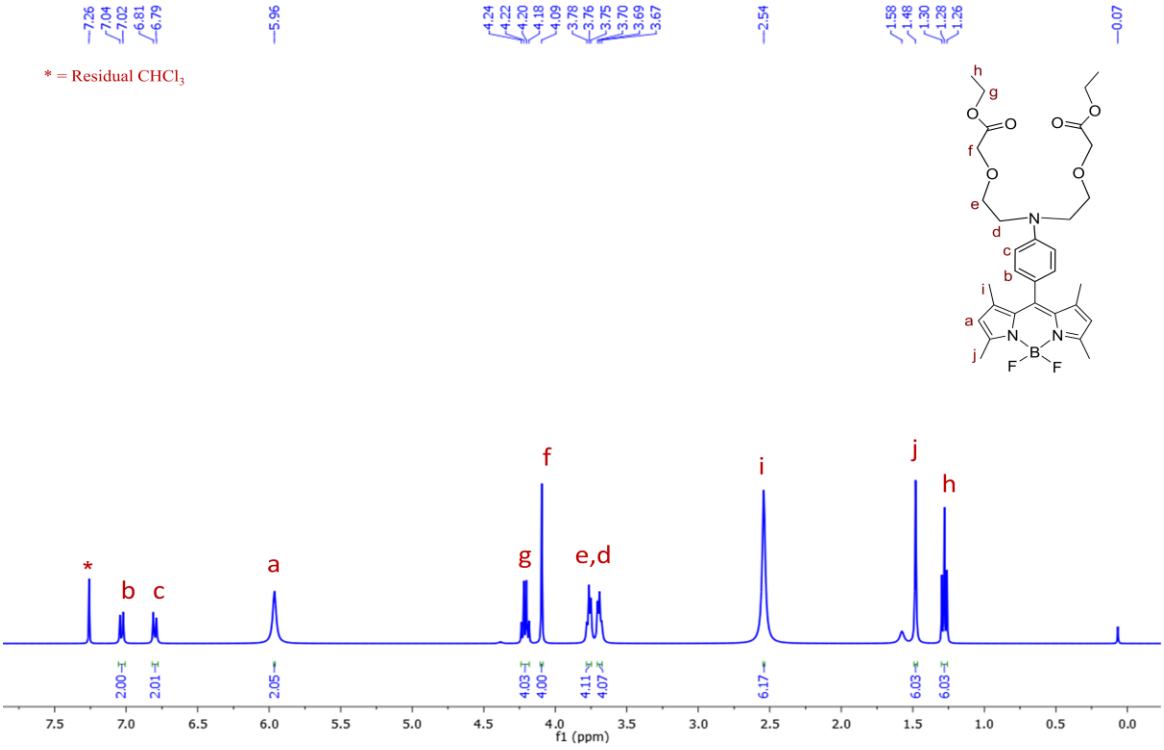

Fig S10: ^{1}H NMR (400 MHz, $CDCl_3$) spectrum of **4**.

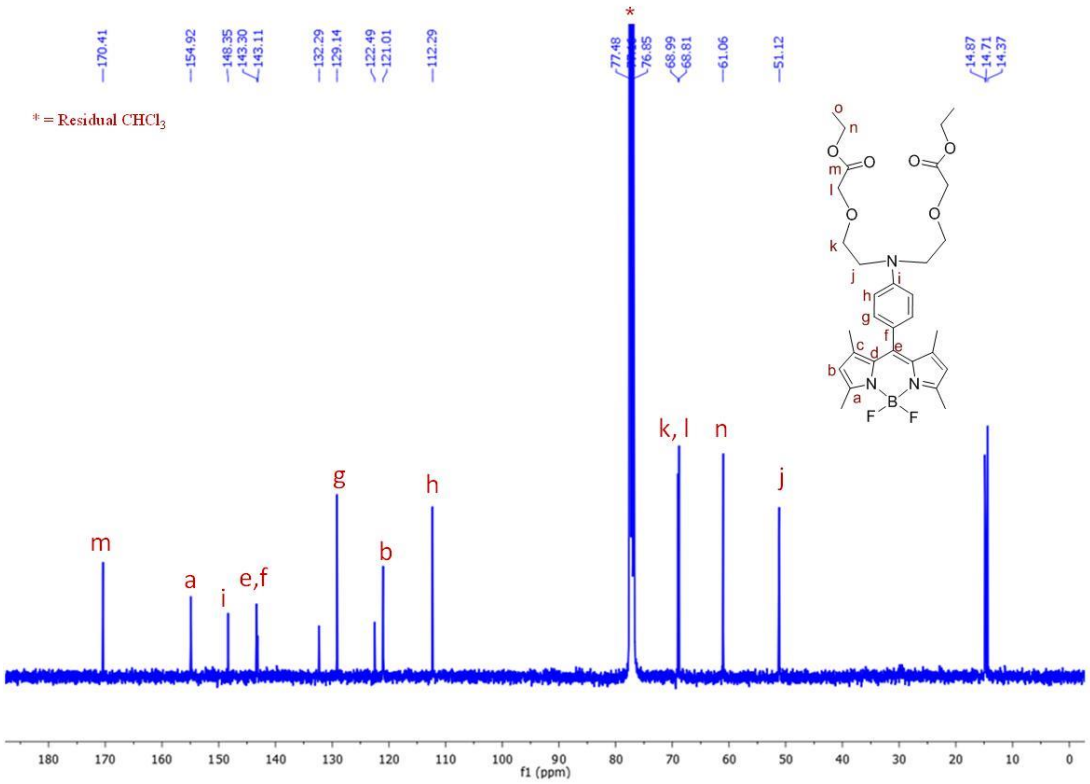

Fig S11: $^{13}C\{^{1}H\}$NMR (100 MHz, $CDCl_3$) spectrum of **4**.

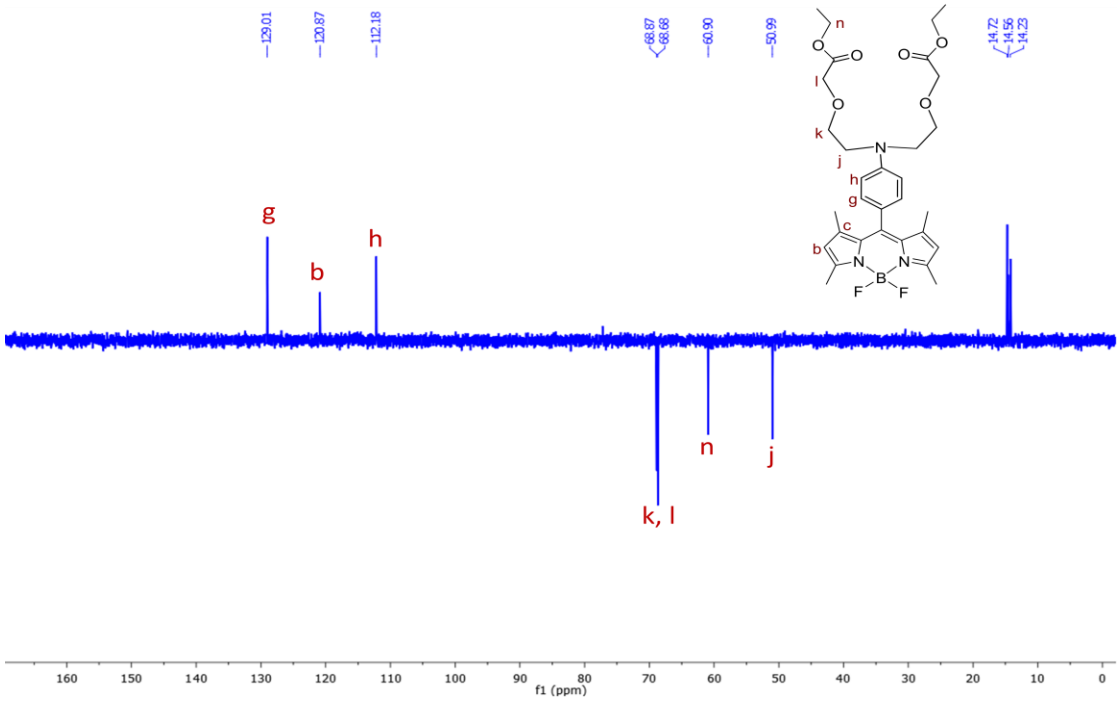

Fig S12: DEPT-135 NMR (100 MHz, $CDCl_3$) spectrum of **4**.

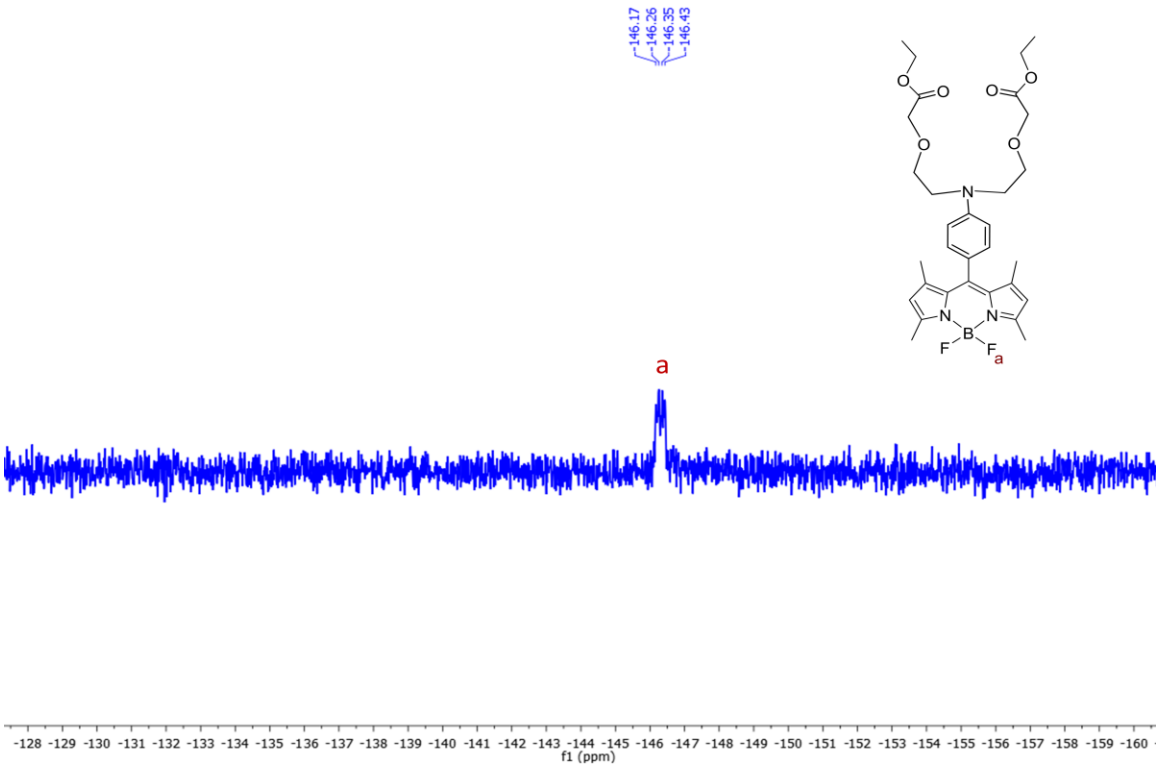

Fig S13: $^{19}F\{^{1}H\}$ NMR (376 MHz, $CDCl_3$) of **4**.

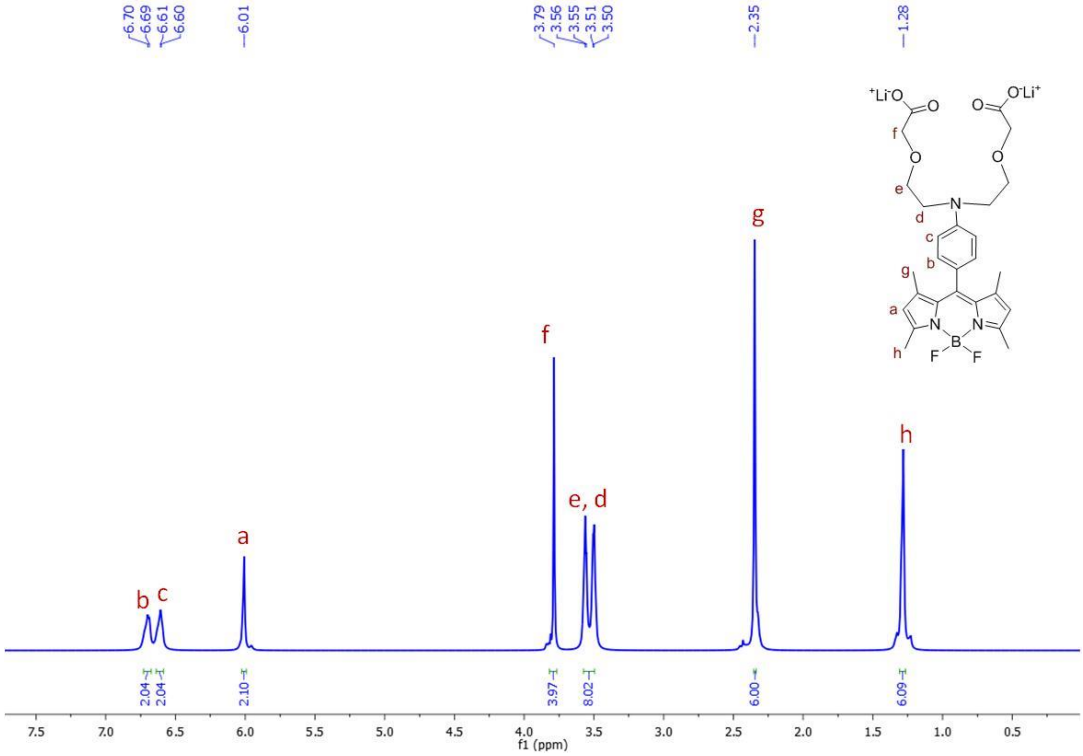

Fig S14: ^{1}H NMR (600 MHz, D_2O) of **LiBDP**.

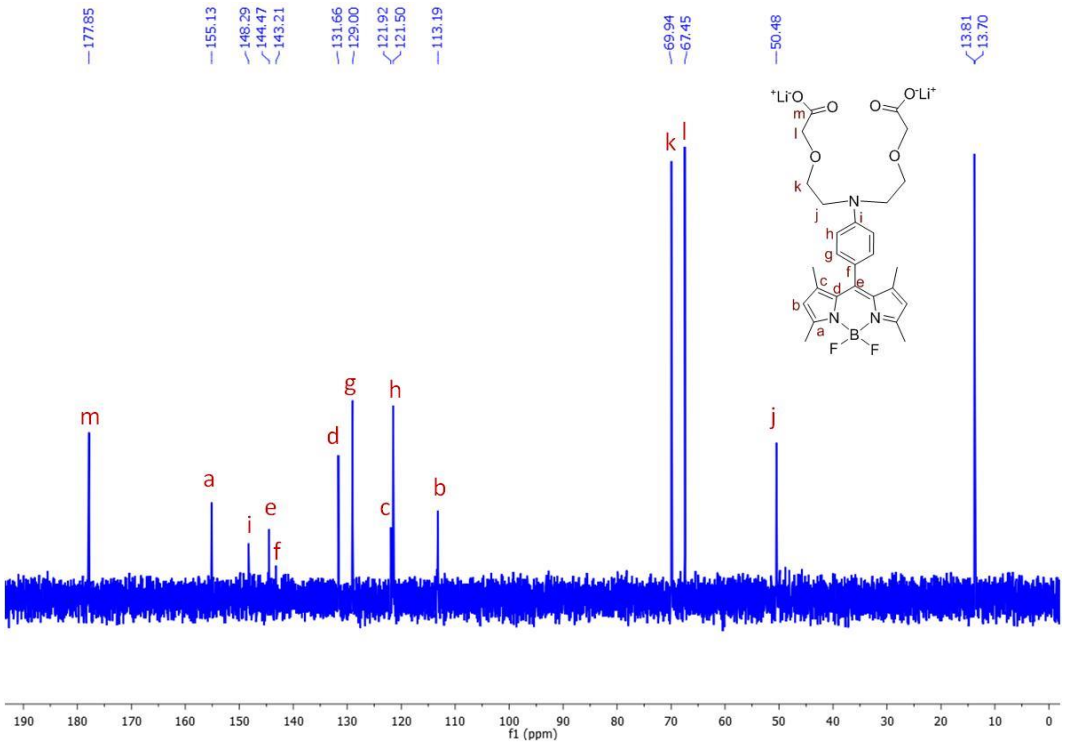

Fig S15: $^{13}C\{^{1}H\}$ NMR (100 MHz, D_2O) of **LiBDP**.

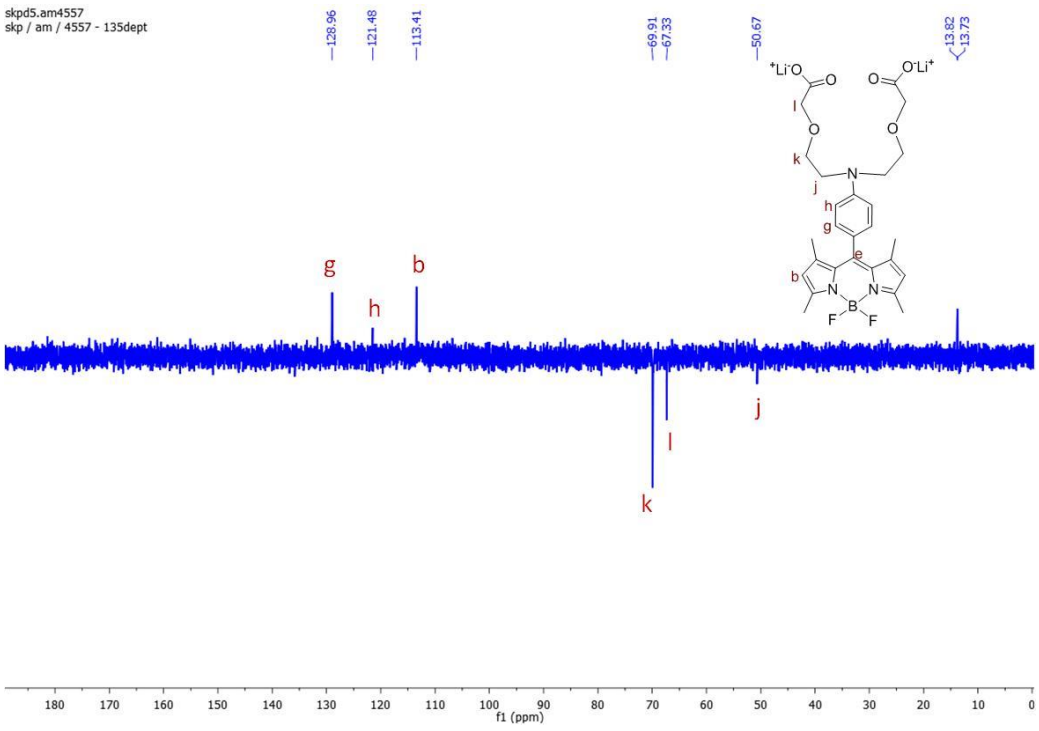

Fig S16: Dept-135 NMR (376 MHz, D_2O) of **LiBDP**.

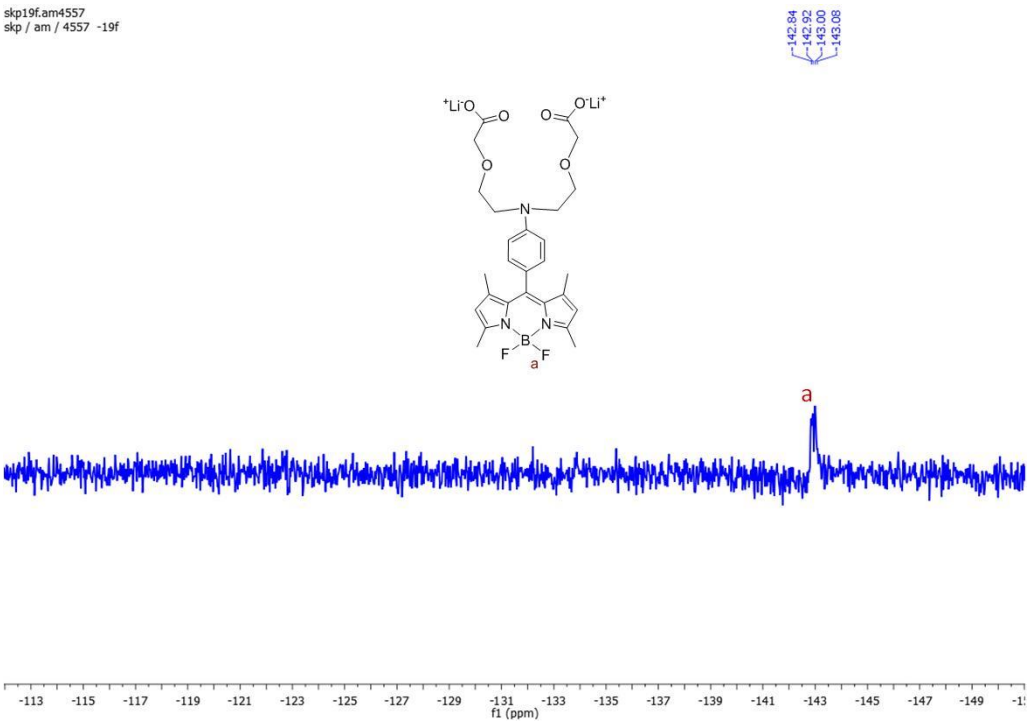

Fig S17: $^{19}F\{^{1}H\}$ NMR (376 MHz, D_2O) of **LiBDP**.

1c. FTIR Spectra

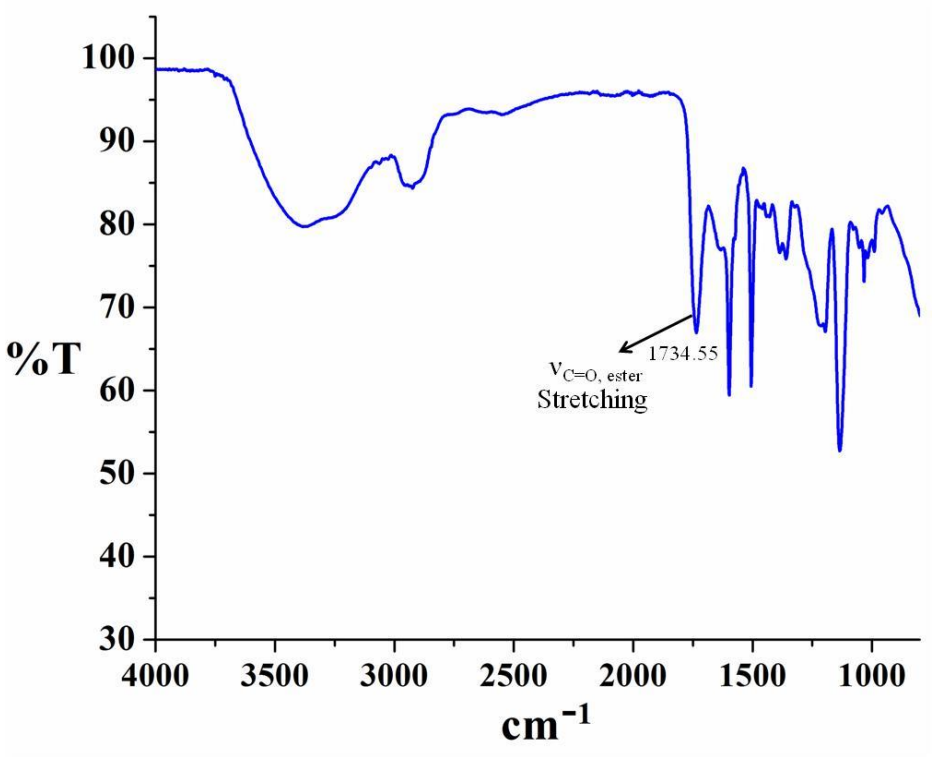

Figure S18. FTIR spectrum of **2.**

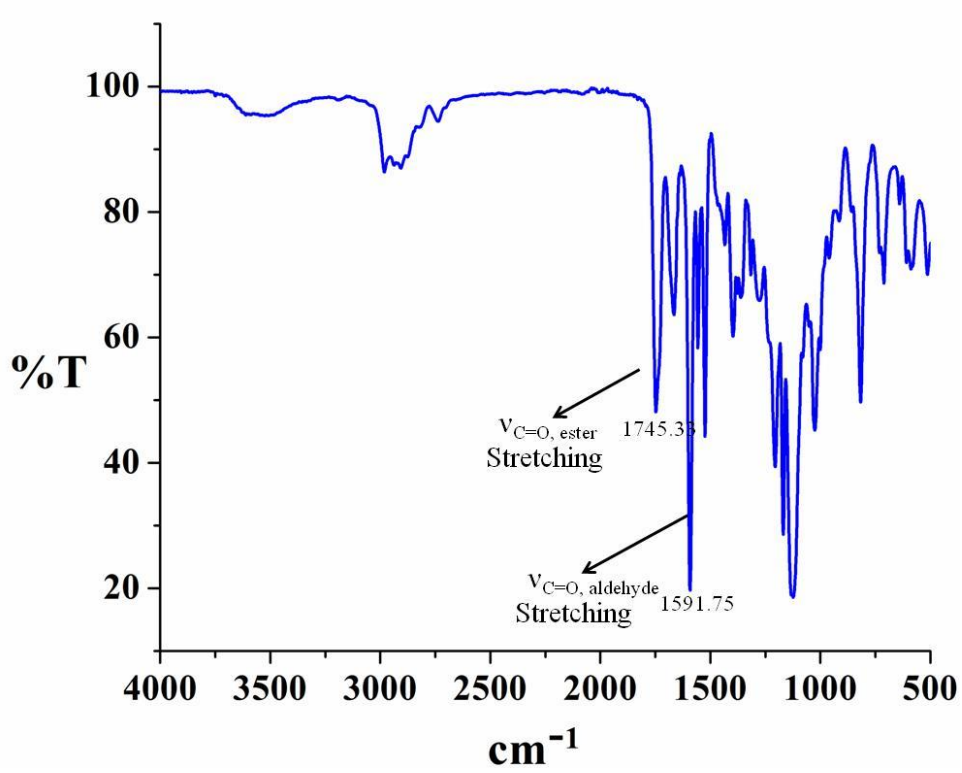

Figure S19. FTIR spectrum of **3.**

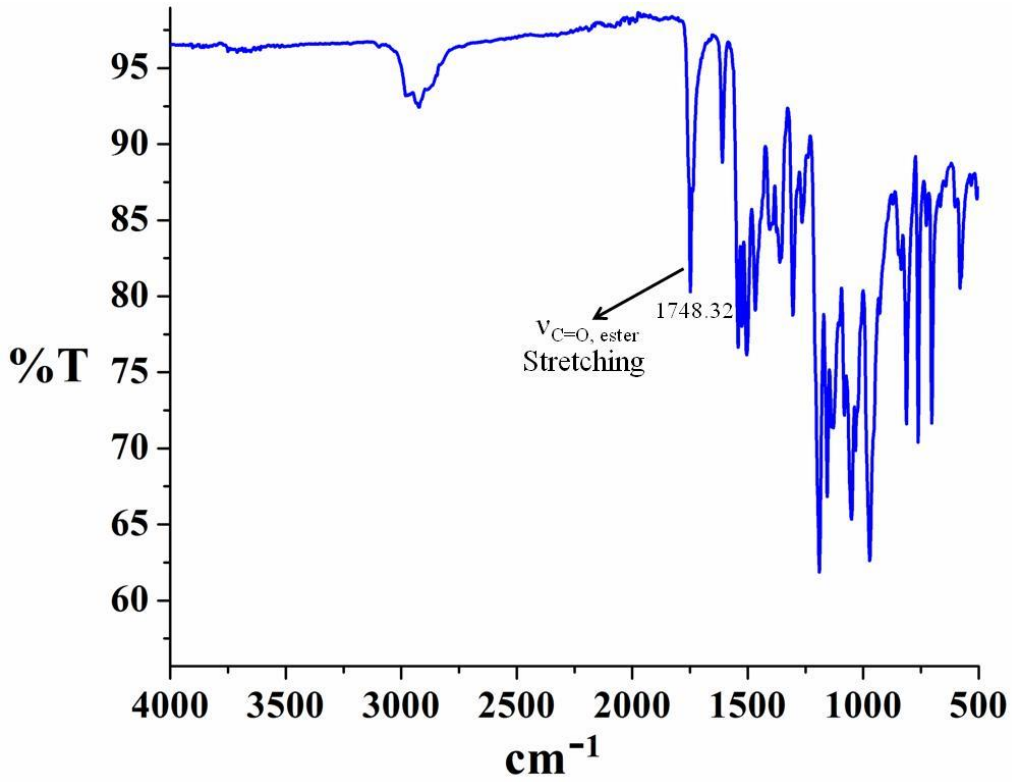

Figure S20. FTIR spectrum of **4.**

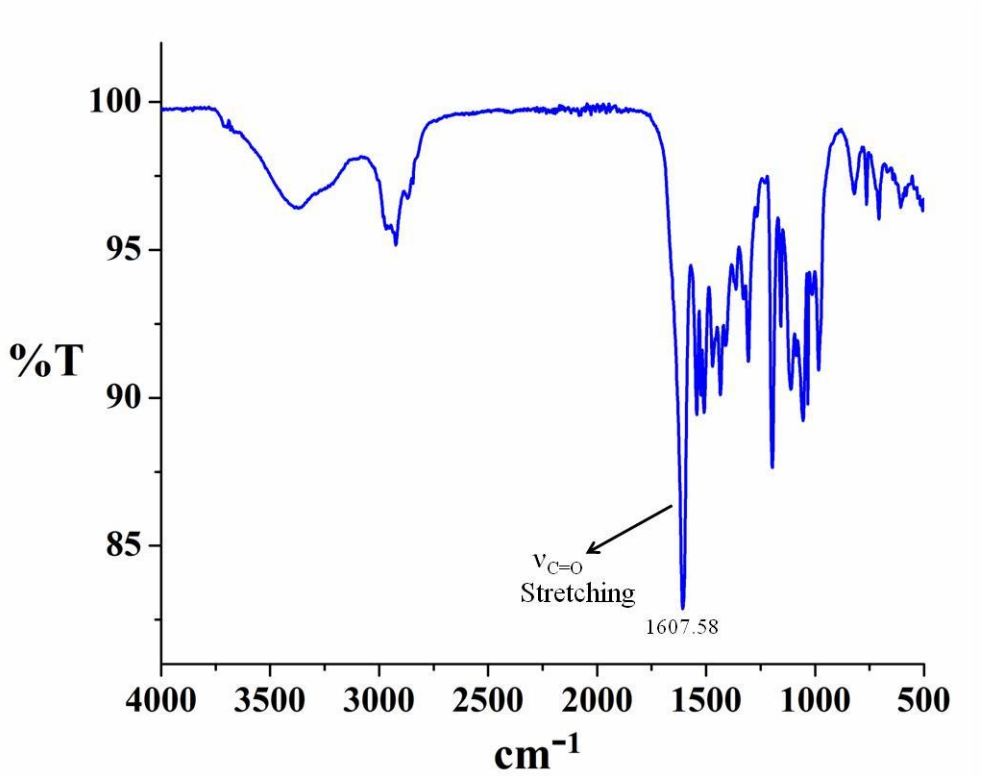

Figure S21. FTIR spectrum of **LiBDP.**

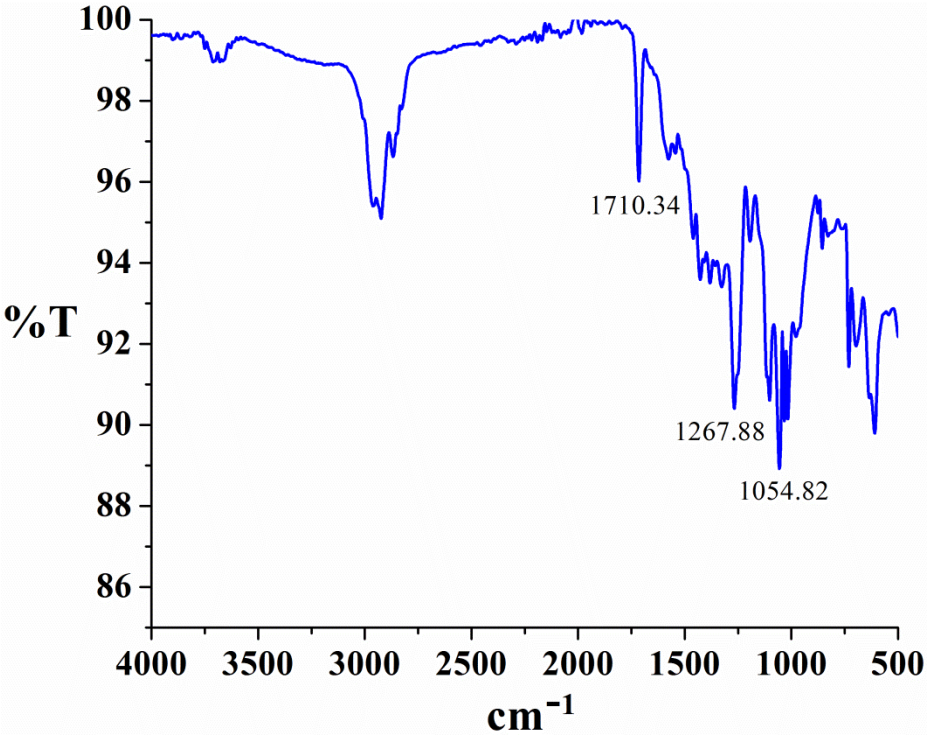

Figure S22. FTIR spectrum of **BDP-Cd(II) complex.**

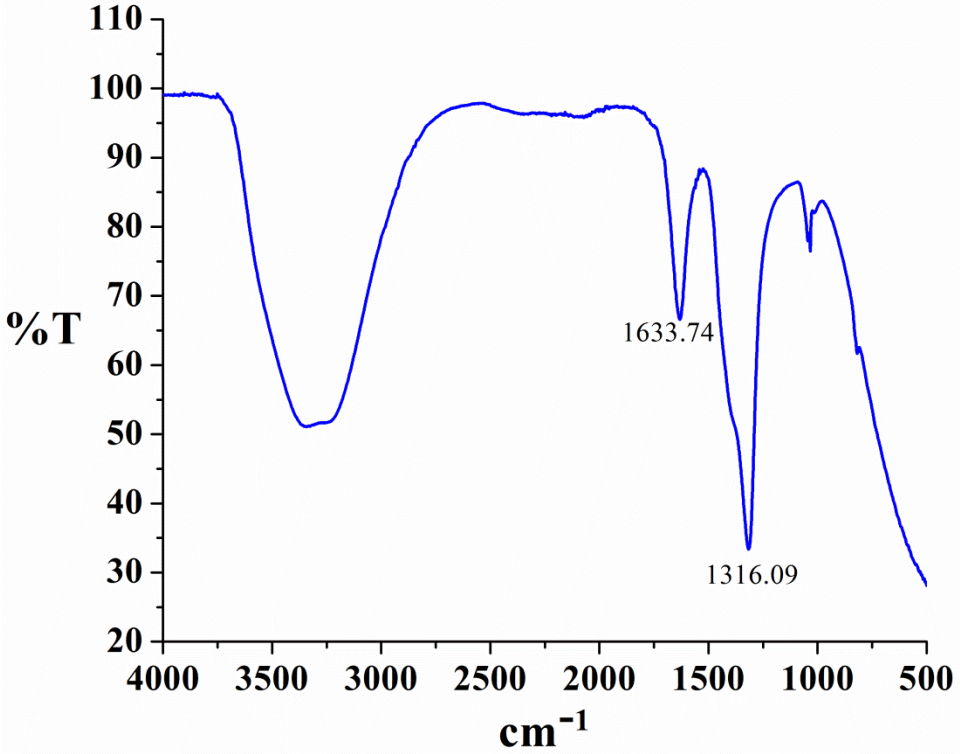

Figure S23. FTIR spectrum of the filtrate containing **$LiNO_3$**.

1d. Mass Data

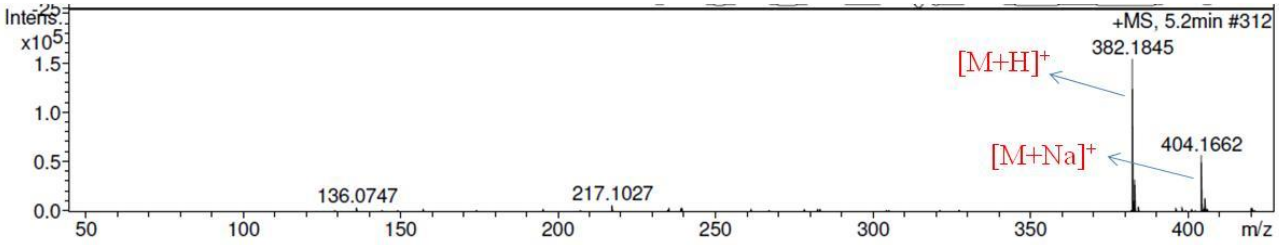

Figure S24. LCMS-HRMS (ESI^+) data of **3.**

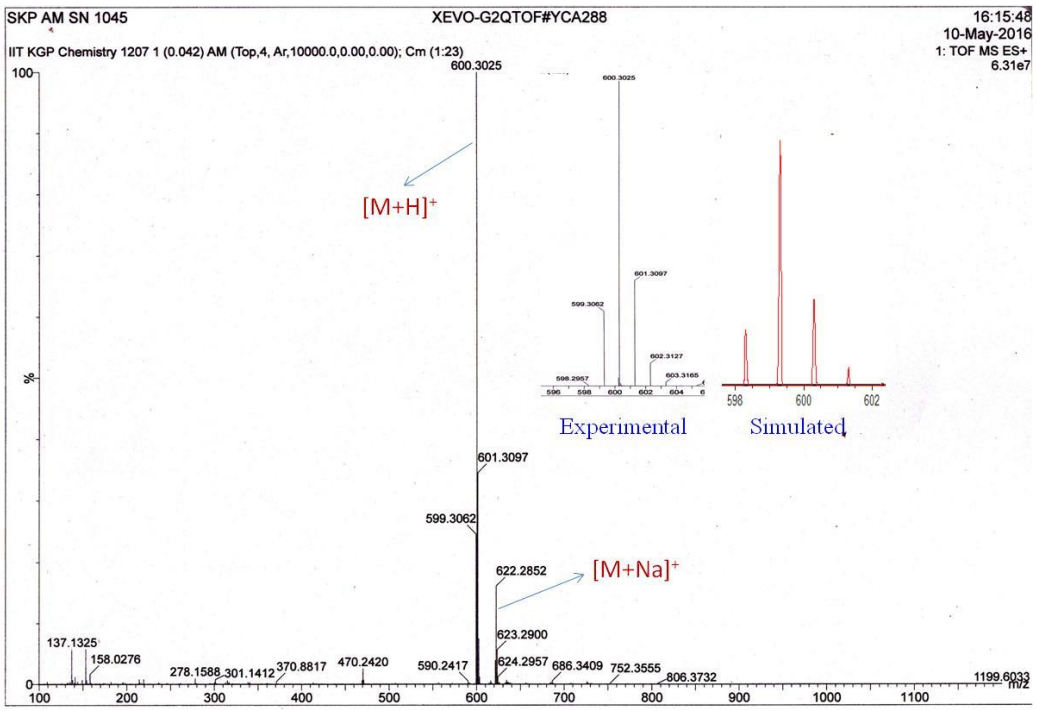

Figure S25. HRMS data of **4** (Inset: Experimental and simulated isotopic distribution at the molecular ion peak).

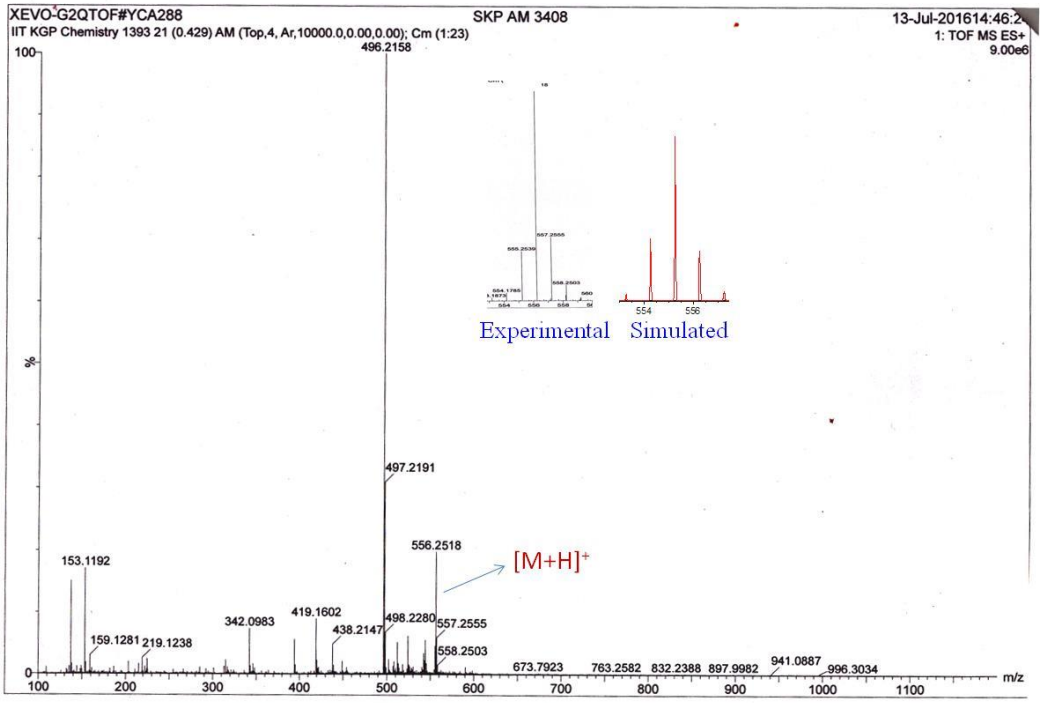

Figure S26. HRMS data of **LiBDP** (Inset: Experimental and simulated isotopic distribution at the molecular ion peak).

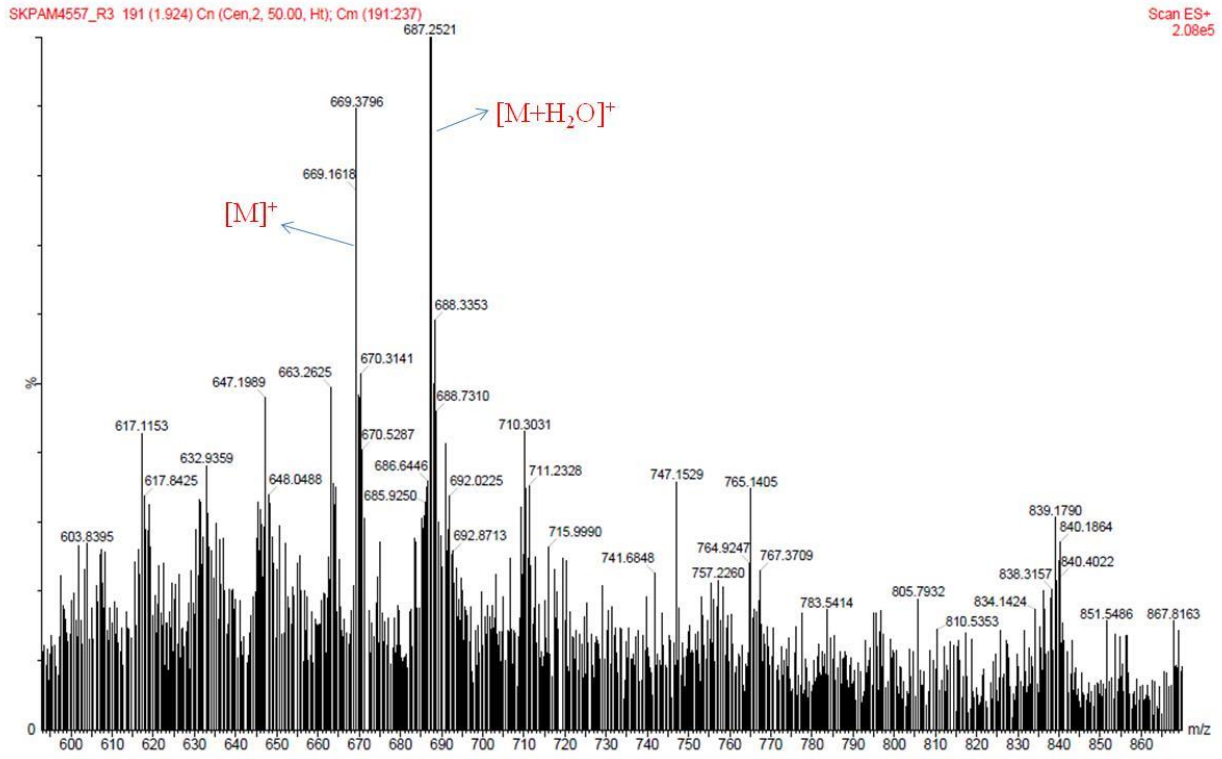

Figure S27. HRMS (ESI^+) data of **LiBDP-Cd^{2+}**.

1.e Synthesis and characterization of BDP-Cd^{2+} complex

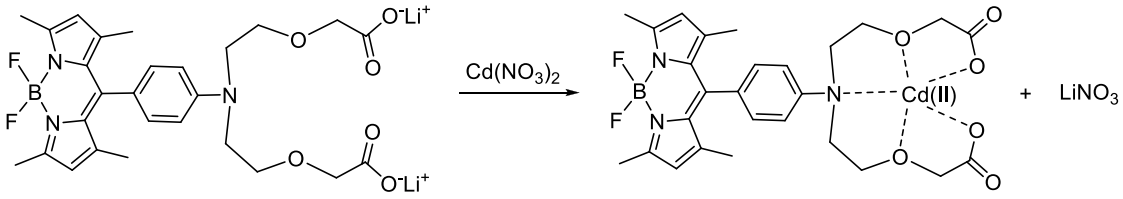

The probe LiBDP (0.05 g, 0.1 mmol) and excess amount of $Cd(NO_3)_2{\cdot}3H_2O$ (0.09 g, 0.3 mmol) was added in distilled H_2O (6 mL) in a round bottom flask, and was allowed to stir at 28 ˚C for 3 hours. The reaction mixture was subjected to centrifuge for 25 minutes and the precipitate formed was filtered off. The residue was washed with distilled water for several times.

Then, both the residue and the filtrate were subjected to FTIR analysis. In the FTIR of the residue, there is no characteristic band for nitrate ions were (Figure S22) whereas, the filtrate showed characteristic bands at 1316 and 1633 cm^{-1} for nitrate ions (Figure S23). Together with mass spectrometry (ESI^+), IR and ^1H NMR analyses, formation of BDP-Cd(II) neutral complex was confirmed.

2. Photophysical and sensing studies

2a. Determination of Quantum yield:

All the UV−Vis absorption and fluorescence emission spectra were collected using a Shimadzu UV−Vis spectrophotometer (model UV 2450) and a Spex Fluorolog-3 spectrofluorimeter (model FL3−11) respectively. Throughout all the measurements, the concentration were maintained at (1×10^{-5}) M. Fluorescence quantum yields were measured with respect to a secondary standard fluorescein in 0.1 M NaOH (Φ = 0.79) at 298 K.[5] The sample and standard concentrations were adjusted to obtain an absorbance of 0.1 or less. The following equation was used to calculate the quantum yields:[6]

$$\frac{\Phi_S}{\Phi_R} = \frac{A_S}{A_R} \times \frac{(Abs)_R}{(Abs)_S} \times \frac{\eta_S^2}{\eta_R^2}$$

Here Φ represents the quantum yield, (Abs) represents the absorbance, A represents the area under the fluorescence curve, and η is the refractive index of H_2O. The subscript S and R denote the corresponding parameters for the sample and reference respectively.

2b. Absorption studies of LiBDP in presence of different metal ions

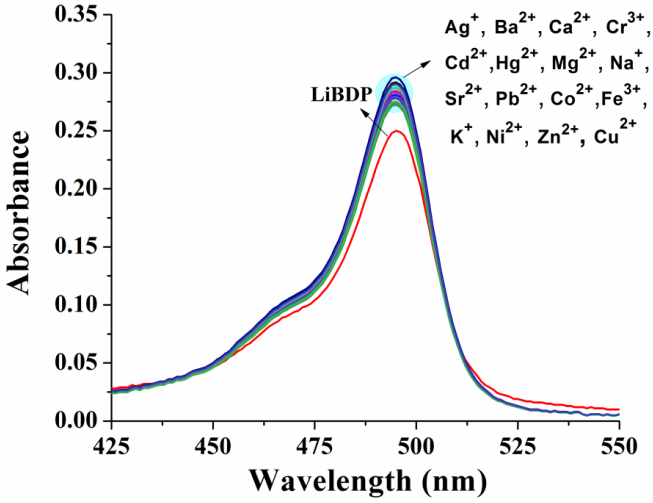

Fig S28: Absorption spectra of **LiBDP** (5μM) upon addition of different metal ions (1 eqv.) in H_2O.

2c. Visual change

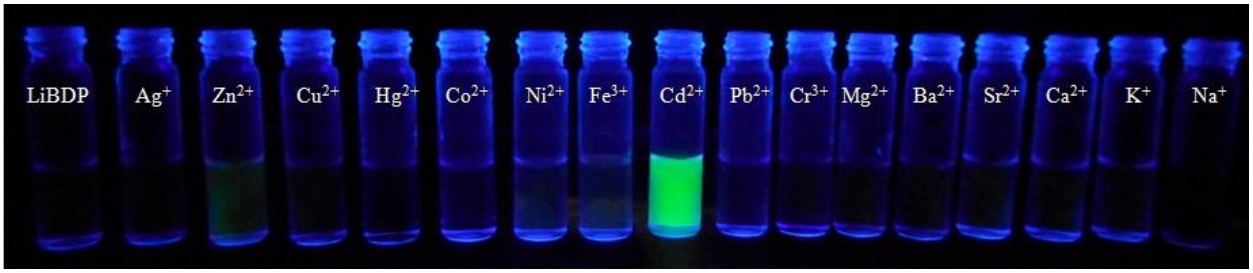

Fig S29: Visual fluorescence changes of **LiBDP** (3×10^{-4} M in H_2O) after addition of different metal ions (1 eqv. with respect to LiBDP) under UV light at 365 nm.

2d. Determination of association constant:

Determination of association constant of **LiBDP** for Cd^{2+}

The association constant was determined by non linear least square fitting of fluorescence intensity versus concentration of Cd^{2+} according to the equation 1:[7]

$$I = I_0 + (I_{lim} - I_0)/2c_0\,[c_0 + c_M + 1/K_s - [(c_0 + c_M + 1/K_s)^2 - 4c_0c_M]^{1/2}]$$

Here, I_0 is the fluorescence intensity of **LiBDP** in the absence of Cd^{2+} and I_{lim} is the maximum fluorescence intensity with Cd^{2+}. K_s is the association constant. c_M is the concentration of Cd^{2+}. I is the fluorescence intensity at any given concentration of Cd^{2+} with **LiBDP**.

2e. Calculation of the limit of detection:

The limit of detection (LOD) of the fluorescent probe **LiBDP** for Cd^{2+} was determined from the following equation:[8]

$LOD = 3\sigma/K$

σ is the standard deviation of the blank solution.

K is the slope of the calibration curve.

From the graph Fig-6 (in the main manuscript), we get slope = 1.72×10^8, and σ value is 10.351. Thus using the formula we get the LOD for $Cd^{2+} = 1.80 \times 10^{-7}$.

Table S1. Comparison of LOD and association constant for the sensing probe **LiBDP** and the reported sensors for the detection of Cd^{2+}.

Reference	**Solvent system**	**LOD (μM)**	**Association constant (M^{-1})**
New J. Chem., 2017, **41**, 14746-14753	3:7 CH_3CN/H_2O	.0584	$1.34 (\pm 0.87) \times 10^6$
Org. Biomol. Chem., 2017, **15**, 2211–2216	1:1 CH_3OH/H_2O	.011	9.06×10^7
Inorg. Chem., 2012, **51**, 9226−9231	C_2H_5OH	-	9.8×10^5
Analyst, 2013, **138**, 1903–1907	1:4 CH_3OH/H_2O	0.1	2.18×10^5
Sensors and Actuators B, 2014, **204**, 474–479.	H_2O	51 ppb	4.9×10^5
J. Fluoresc, 2017, **27**,1871–1875	9:1 CH_3OH/H_2O	0.047	-
Inorg. Chem., 2011, **50**, 10041–10046	CH_2Cl_2/CH_3CN (1:9)	-	3.7×10^4
Inorg. Chem., 2014, **53**, 12665−12667	EtOH/H_2O (1:1)	5.57	1.4×10^4
Analyst, 2013, **138**, 901–906	1:1 CH_3CN/HEPES	0.048	9.45×10^6
Spectrochimica Acta Part A: Molecular and Biomolecular Spectroscopy, 2016, **163**, 120–126	C_2H_5OH	0.276	-
Dalton Trans., 2015, **44**, 104–109	DMF–H_2O (1 : 1)	0.010	$(7.7 \pm 0.8) \times 10^6$
Org. Biomol. Chem., 2013, **11**, 3014-3019	CH_3CN–HEPES buffer (1 : 1)	0.219	5.59×10^5
Chem. Asian J. 2013, **8**, 1441 – 1446	CH_3CN		$4.4 (\pm 0.9) \times 10^4$
J. Am. Chem. Soc. **2008**, 130, 16160–16161	Tris-HCl (0.02 M)	-	7.2×10^3
Org. Lett, 2007, **9**, 3829-3832	50 mM HEPES	-	$(8.14 \pm 3.01) \times 10^6$
Chem. Eur. J., 2010, **16**, 919–930	MeCN/H2O (1:1	-	$\sim 10^6$
Our probe (In this work)	H_2O	0.18	$2.57 \pm 1.06 \times 10^5$

2f. pH dependency study

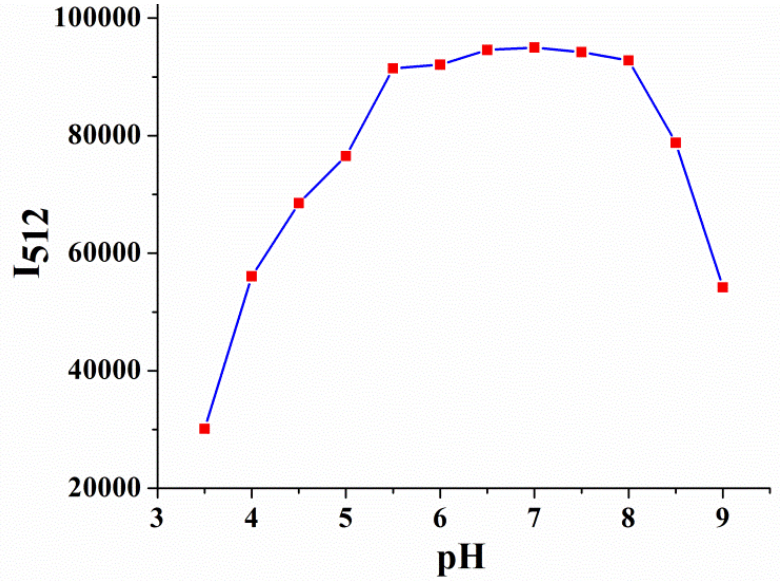

Fig S30: Relative fluorescence intensity of **LiBDP** at various pH values exhibiting the operational pH range of 5.5 to 8.

2g. Anion sensitivity study

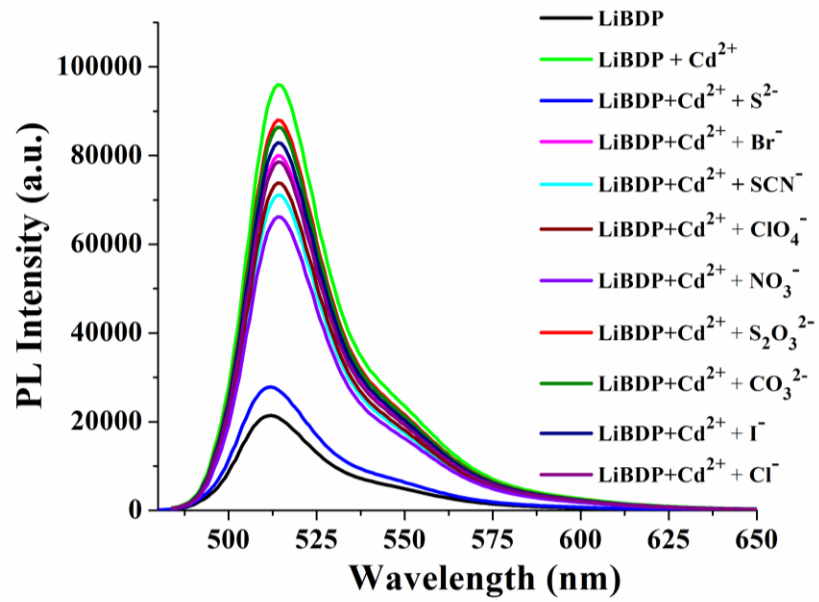

Fig S31: Emission spectra of **LiBDP** (5×10^{-6} M) upon addition of 1 equiv. of Cd^{2+} followed by various anions.

2h. Reversibility studies of BDP-Cd^{2+} by continuous variation of S^{2-} ion concentration

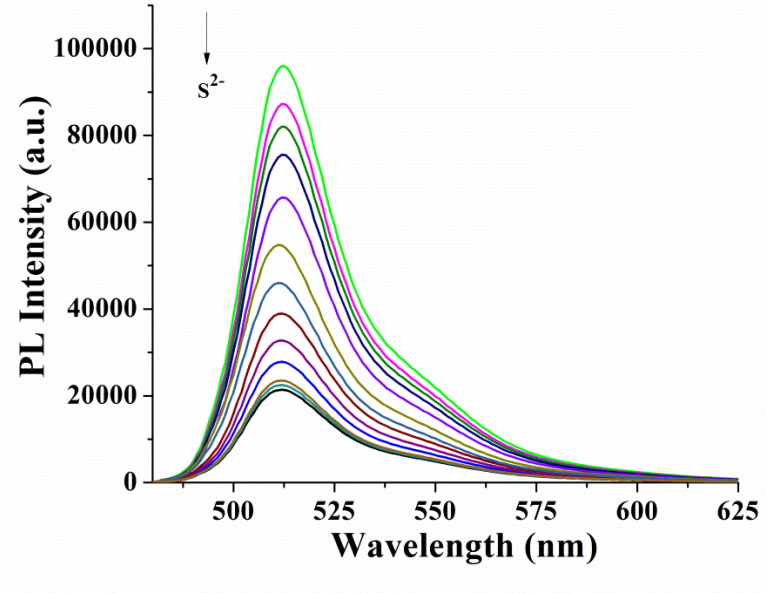

Fig S32: Fluorescence recovery responses of **LiBDP-Cd^{2+}** (5μM in H_2O) upon successive addition of S^{2-}.

2i. Preparation of LiBDP test paper:

Test papers of **LiBDP** were prepared by dipping the pieces of filter paper (Whatman 41) in MeOH (1 mM) solution of **LiBDP,** and then dried in air. The test papers coated with **LiBDP** were then immersed to the various concentrations of Cd^{2+} (0.1 μM to 100 μM). After dipping the test paper (**LiBDP**) color changed from light red to increasing intensity of green fluorescence which can be detected by naked eye (under UV illumination at 365 nm) as shown in Fig. 9 in the main manuscript.

2j. Cell imaging study:

Chronic myeloid leukemia cells (K562) were procured from National Centre for Cell Science, Pune, India. Cells were cultured in RPMI 1640 media supplemented with 10% fetal bovine serum and maintained in a humidified incubator with 5% CO_2 and at 37 ˚C. The fluorescence imaging of K562 cells with **LiBDP** and followed by the addition of Cd^{2+} was observed under confocal microscope imaging system (FV 1000, Olympus, Japan).

2k. Computational details:

The density functional theory (DFT) calculation and geometry optimization was carried out using the Gaussian 09 program based on Becke's three-parameter set with Lee-Yang-Parr correlation functional (B3LYP).[9] The LanL2DZ (Los-Alamos National Laboratory (LANL) effective core potentials to describe the core electrons together with the split valence double-zeta) basis set was employed for Cd element while the 6-31G(d,p) basis set was assigned to other elements (C, H, B, N Li and F).

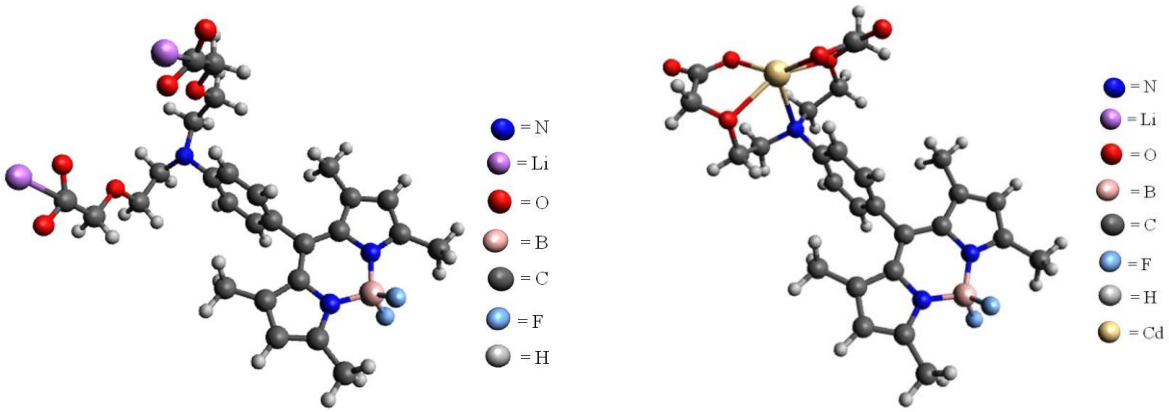

Fig S33: Optimized geometry of model probe molecule **LiBDP** (Left) and proposed Cd^{2+}-coordination (Right) obtained from DFT computed optimized structure.

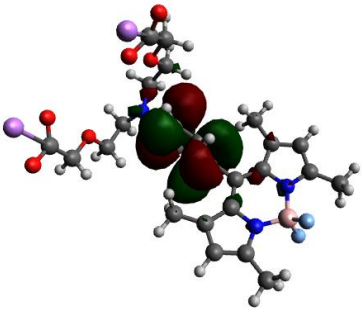

LUMO+2 = -1.058 eV

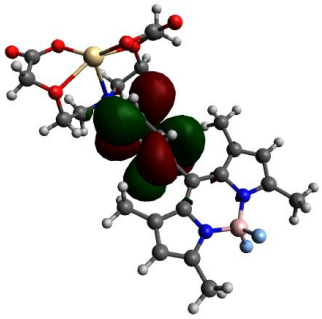

LUMO+2 = -1.622 eV

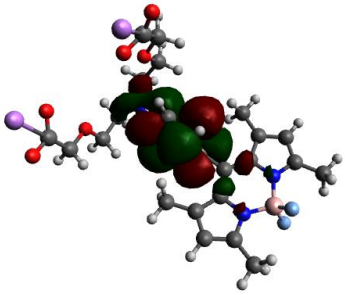

LUMO+1 = -1.279 eV

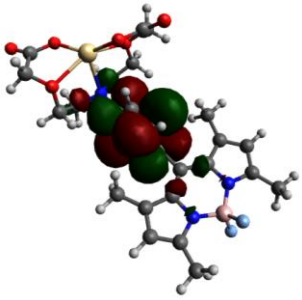

LUMO+1 = -1.748 eV

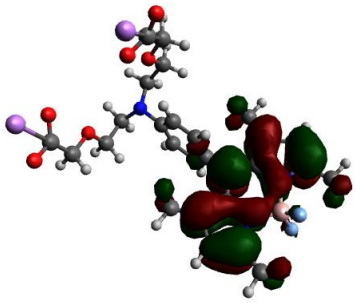

LUMO = -2.158 eV

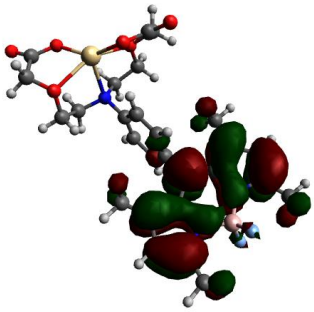

LUMO = -3.095 eV

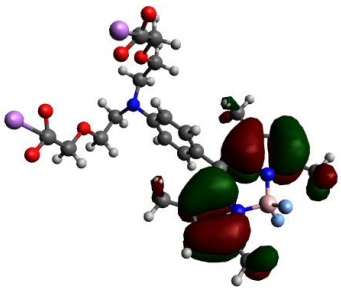

HOMO = -5.166 eV

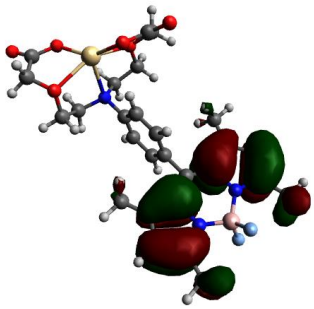

HOMO = -6.056 eV

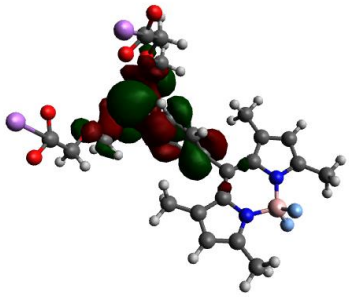

HOMO-1 = -5.385 eV

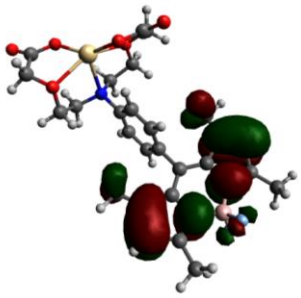

HOMO-1 = -6.719 eV

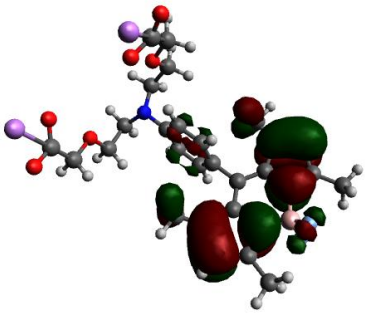

HOMO-2 = -6.242 eV

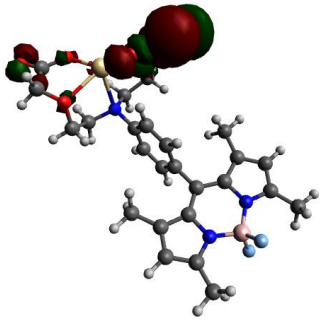

HOMO-2 = -6.758 eV

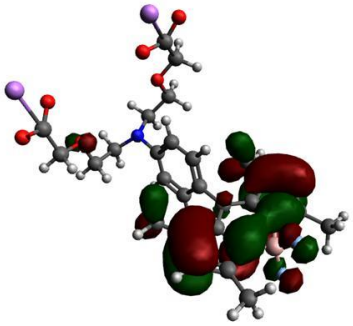

HOMO-3 = -6.448 eV

LiBDP

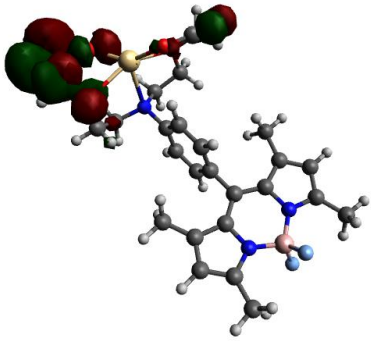

HOMO-3 = -7.132 eV

[**BDP-Cd**$^{2+}$]

Fig. S34: Selected Frontier Molecular Orbitals (FMOs) of **LiBDP** and [**BDP·Cd(II)**] complex, estimated from DFT calculations.

3. References

1. X. Shen, H. Liu, Y. Li and S. Liu, *Macromolecules*, 2008, **41**, 2421.
2. X. Jiang, C. Wong, P. Lo and D. K. P. Ng, *Dalton Trans*., 2012, **41**, 1801.
3. G. Meng, M. L. Zheng and M. Wang, *org. prep. proced. Int.*, 2011, **43**, 308.

4. Y. He, M. Lin, Z. Li, X. Liang, G. Li and J. C. Antilla, *Org. Lett.*, 2011, **13**, 4490.
5. J. Q. Umberger, and V. K. Lamer, *J. Am. Chem. Soc.*, 1945, **67**, 1099.
6. A. Chakraborty, D. Chakrabarty, P. Hazra, D. Seth and N. Sarkar, *Chem. Phys. Lett*., 2003, **382**, 508.
7. (a) V. P Singh, K. Tiwari, M. Mishra, N. Srivastava and S. Saha, *Sens. Actuators, B*, 2013, **182**, 546. (b) J. Bourson, J. Pouget and B. Valeur, *J. Phys. Chem.*, 1993, **97**, 4552.
8. (a) IUPAC commission on spectrochemical and other optical procedures for analysis, *Pure. Appl. Chem.*, 1976, **45**, 107. (b) Y. Chen, C. Zhu, J. Yang, J. Li, Y. Jiao, W. He, J. Chen and Z. Guo, *Chem. Commun.*, 2012, **48**, 5094. (c) B. In, G. W. Hwang and K. Lee, *Bioorg. Med. Chem. Lett*., 2016, **26**, 4477.
9. (a) M. J. Frisch, G. W. Trucks, H. B. Schlegel, G. E. Scuseria, M. A. Robb, J. R. Cheeseman, G. Scalmani, V. Barone, B. Mennucci, G. A. Petersson, H. Nakatsuji, M. Caricato, X. Li, H. P. Hratchian, A. F. Izmaylov, J. Bloino, G. Zheng, J. L. Sonnenberg, M. Hada, M. Ehara, K. Toyota, R. Fukuda, J. Hasegawa, M. Ishida, T. Nakajima, Y. Honda, O. Kitao, H. Nakai, T. Vreven, J. A. Montgomery Jr., J. E. Peralta, F. Ogliaro, M. Bearpark, J. J. Heyd, E. Brothers, K. N. Kudin, V. N. Staroverov, R. Kobayashi, J. Normand, K. Raghavachari, A. Rendell, J. C. Burant, S. S. Iyengar, J. Tomasi, M. Cossi, N. Rega, J. M. Millam, M. Klene, J. E. Knox, J. B. Cross, V. Bakken, C. Adamo, J. Jaramillo, R. Gomperts, R. E. Stratmann, O. Yazyev, A. J. Austin, R. Cammi, C. Pomelli, J. W. Ochterski, R. L. Martin, K. Morokuma, V. G. Zakrzewski, G. A. Voth, P. Salvador, J. J. Dannenberg, S. Dapprich, A. D. Daniels, Ö. Farkas, J. B. Foresman, J. V. Ortiz, J. Cioslowski and D. J. Fox, Gaussian 09, Gaussian Inc., Wallingford, CT, 2009. (b) M. Reiher, O. Salomon and B. A. Hess, *Theor. Chem. Acc.* 2001, **107**, 48.